

An Innovative Experiment to Test a Paradigm-Shifting Theory in Physics through Alteration of Light Speed in Electromagnetic Interactions

Wim Vegt
Department of Physics
Eindhoven University of Technology
The Netherlands
wimvegt@quantumlight.science



Abstract

Within the realm of astronomy and astrophysics, the profound connections between Black Holes, Dark Matter, and the intricate interplay among light, gravity, and electromagnetic forces continue to captivate researchers. Building upon the foundational tenets of Einstein's General Relativity, which elucidate the curvature of spacetime under the influence of gravitational fields and uphold the constant speed of light in vacuum, a fresh perspective emerges.

This novel viewpoint pivots on the concept of "Equilibrium" governing the five fundamental force densities in light, suggesting dynamic variations in light speeds when coherent laser beams intersect. This departure from the conventional assumption of a constant light speed challenges the core principles, [Einstein Albert \(1953\)](#), of General Relativity, prompting a thorough investigation into the gravitational and luminous interactions at both celestial and sub-atomic scales. The exploration extends across diverse phenomena, encompassing Gravitational Redshift, Black Holes, Dark Matter, and the intricate processes of light absorption and emission on a microscopic scale.

In contrast to the established framework of General Relativity, this innovative perspective seeks to merge the realms of gravity and light through a harmonious amalgamation of the Stress-Energy Tensor and the Gravitational Tensor. This union not only sheds light on the nuanced interplay between gravity and electromagnetism but also unveils a novel tensor representation for Black Holes termed as Gravitational Electromagnetic Confinements. By integrating electromagnetic energy gradients and Lorentz transformations, this approach transcends the traditional boundaries of General Relativity, particularly evident in scenarios of Gravitational Lensing.

The reinterpretation of Einstein's foundational work, [Einstein Albert \(June 21, 1911\)](#), featuring the Einstein Gravitational Constant within the Energy-Stress Tensor, introduces a combined Electromagnetic Tensor and Gravitational Tensor framework. Theoretical advancements in Black Hole solutions resonate with the pioneering spirit of Jonh Archibald Wheeler's work in 1955, providing essential solutions for the relativistic quantum mechanical Dirac equation within a tensor formalism. Experimental validation of this paradigm shift, combining data from Galileo Satellites and ground-based MASER frequency measurements, underscores the disparities between General Relativity and the proposed New Theory, pushing the boundaries of gravitational observations to unprecedented accuracies.

The synergy between Quantum Physics and General Relativity theories, as exemplified by approaches like String Theory, anticipates variances in natural constants. This interdisciplinary pursuit aims to redefine our understanding of the gravitational constant "G," illuminating its timeless constancy while bridging the domains of General Relativity and Quantum Physics.

This abstract encapsulates the essence of groundbreaking research unfolding at the intersection of light, gravity, and theoretical frameworks within the realm of astronomy and astrophysics, offering tantalizing prospects for transformative discoveries at the forefront of optical and gravitational sciences.

Keywords

Black Holes, Dark Matter, Light Speed Variability, Gravity, Electromagnetic Forces, General Relativity, Equilibrium Principle, Gravitational Redshift, Stress-Energy Tensor, Gravitational Electromagnetic Interaction, Lorentz Transformations, Gravitational Lensing, Quantum Physics, String Theory

1. Gravity

Einstein approached the interaction between gravity and light by the introduction of the “Einstein Gravitational Constant” in the 4-dimensional Energy-Stress Tensor.

$$G_{\mu\nu} + \Lambda g_{\mu\nu} = \kappa T_{\mu\nu} \quad (1)$$

In which $G_{\mu\nu}$ equals the Einstein Tensor, $g_{\mu\nu}$ equals the Metric Tensor, $T_{\mu\nu}$ equals the Stress-Energy tensor, Λ equals the cosmological constant and κ equals the Einstein gravitational constant.

The core principle underlying General Relativity pertains to a curved 4-dimensional Space-Time Continuum. Similarly, the fundamental concept in this novel theory revolves around a 4-dimensional Universal Equilibrium delineated by equation (6).

Central to this novel theory is the vectorial summation of force densities denoted in $[N/m^3]$. Force densities hold universal significance and are interchangeable irrespective of their source. [Vegt Wim \(1995\)](#) Within this framework, fields solely engage with analogous fields. The theory contemplates three distinct categories of physical fields: Electric Fields, Magnetic Fields, and Gravitational Fields.

The outcome of the interaction between two corresponding fields manifests as a force density articulated in $[N/m^3]$. When two electric fields interact, the resultant force density is an electric force density delineated in $[N/m^3]$. Similarly, the convergence of two magnetic fields yields a magnetic force density expressed in $[N/m^3]$. Likewise, the intersection of two gravitational fields produces a gravitational force density expressed in $[N/m^3]$. At the core of this theory lies the foundational principle that all force densities collectively establish a universal equilibrium. This elucidation can be found in Reference [10], specifically detailed within equations (4) through (22).

The vectorial force densities are derived from the divergence of the sum of the Electromagnetic Stress-Energy tensor $\overset{=}{T}$ and a selected Gravitational Tensor $\overset{=}{J}$.

$$\kappa T_{\mu\nu} \Leftrightarrow \overset{=}{T}_{\mu\nu} + \overset{=}{J}_{\mu\nu} \quad (2)$$

The 4-dimensional divergence of the sum of the Electromagnetic Stress-Energy tensor and the Gravitational Tensor expresses the 4-dimensional Force-Density vector (expressed in $[N/m^3]$ in the 3 spatial coordinates) as the result of Electro-Magnetic-Gravitational interaction.

$$f^{\mu} = \partial_{\nu} \left(T^{\mu\nu} + J^{\mu\nu} \right) \quad (3)$$

In vector notation the 4-dimensional Force-Density vector can be written as:

$$\vec{f}^4 = \begin{pmatrix} f_4 \\ f_3 \\ f_2 \\ f_1 \end{pmatrix} = \square \cdot \left(\vec{T} + \vec{J} \right) \quad (4)$$

The fundamental boundary condition for this alternative approach to gravity is the requirement that the Force 4 vector equals zero in the 4 dimensions, expressing a universal 4-dimensional equilibrium [Vegt Wim \(1995\)](#):

$$\vec{f}^4 = \begin{pmatrix} f_4 \\ f_3 \\ f_2 \\ f_1 \end{pmatrix} = \square \cdot \left(\vec{T} + \vec{J} \right) = \vec{0} \quad (5)$$

Within this innovative framework, the interactions among electric-electric fields, magnetic-magnetic fields, and gravitational-gravitational fields are interchangeable. Consequently, the gravitational force density mirrors a comparable structure to that of the electric force density and the magnetic force density. The three spatial components of the Force-Density vector arising from the Electro-Magnetic-Gravitational interaction can be expressed as:

$$\begin{aligned} \bar{f} = & -\frac{1}{c^2} \frac{\partial (\bar{\mathbf{E}} \times \bar{\mathbf{H}})}{\partial t} + \varepsilon_0 \bar{\mathbf{E}} (\nabla \cdot \bar{\mathbf{E}}) - \varepsilon_0 \bar{\mathbf{E}} \times (\nabla \times \bar{\mathbf{E}}) + \\ & + \mu_0 \bar{\mathbf{H}} (\nabla \cdot \bar{\mathbf{H}}) - \mu_0 \bar{\mathbf{H}} \times (\nabla \times \bar{\mathbf{H}}) + \gamma_0 \bar{\mathbf{g}} (\nabla \cdot \bar{\mathbf{g}}) - \gamma_0 \bar{\mathbf{g}} \times (\nabla \times \bar{\mathbf{g}}) = \bar{0} \quad [\text{N/m}^3] \end{aligned} \quad (6)$$

in which: $\mu_0 (\nabla \cdot \bar{\mathbf{H}}) = \rho_M$ Magnetic Flux Density [Vs/ m³] or [Wb/ m³]

$\gamma_0 (\nabla \cdot \bar{\mathbf{g}}) = \rho_M$ Mass Density (Electromagnetic) [kg/ m³]

Electric Energy Density: $w_E = \frac{1}{2} \varepsilon_0 E^2$

Magnetic Energy Density: $w_M = \frac{1}{2} \mu_0 H^2$

Gravitational Energy Density: $w_G = \frac{1}{2} \gamma_0 g^2$

In which E represents the electric field intensity expressed in [V/m], H represents the magnetic field intensity expressed in [A/m] and g represents the gravitational acceleration expressed in [m/s²]. The permittivity indicated as, ε_0 the permeability indicated as μ_0 and the gravitational permeability of vacuum as γ_0 .

The initial term in equation (6) portrays the inertia inherent in electromagnetic radiation, while the succeeding terms, two and three, denote the interaction between electric fields. Subsequently, the fourth and fifth terms represent the interaction of magnetic fields, and the sixth and seventh terms pertain to gravitational field interactions.

At the heart of this newly suggested theory resides a fundamental notion of universal equilibrium, demonstrating a pervasive presence across temporal, directional, and spatial dimensions. This overarching equilibrium finds concise representation through the zero-vector placed on the right-hand side of the equality symbol. An instance illustrating three-dimensional universal equilibrium is akin to the projection of a slide onto a screen [4].

In the realm of curl-free gravitational fields [23], equation (6) is identical to equation (22) delineated in References [10] and [16]. In the context of curl-free gravitational fields [Weng Zihua, \(October 2008\)](#), equation (6) may be reformulated as follows:

$$\begin{aligned} \bar{f} = & -\frac{1}{c^2} \frac{\partial (\bar{\mathbf{E}} \times \bar{\mathbf{H}})}{\partial t} + \varepsilon_0 \bar{\mathbf{E}} (\nabla \cdot \bar{\mathbf{E}}) - \varepsilon_0 \bar{\mathbf{E}} \times (\nabla \times \bar{\mathbf{E}}) + \\ & + \mu_0 \bar{\mathbf{H}} (\nabla \cdot \bar{\mathbf{H}}) - \mu_0 \bar{\mathbf{H}} \times (\nabla \times \bar{\mathbf{H}}) + \bar{g} \rho_M = \bar{0} \quad [\text{N/m}^3] \end{aligned} \quad (7)$$

Substituting Einstein's $W = m c^2$ in (7) results in “Electro-Magnetic-Gravitational Equilibrium Field Equation” (8) [Vegt Wim \(2 Oct, 2021\)](#) , [Vegt Wim \(14 October 2022\)](#) and [Vegt Wim \(26-Oct-2022\)](#):

$$\begin{aligned} \bar{f} = & -\frac{1}{c^2} \frac{\partial (\bar{\mathbf{E}} \times \bar{\mathbf{H}})}{\partial t} + \varepsilon_0 \bar{\mathbf{E}} (\nabla \cdot \bar{\mathbf{E}}) - \varepsilon_0 \bar{\mathbf{E}} \times (\nabla \times \bar{\mathbf{E}}) + \\ & + \mu_0 \bar{\mathbf{H}} (\nabla \cdot \bar{\mathbf{H}}) - \mu_0 \bar{\mathbf{H}} \times (\nabla \times \bar{\mathbf{H}}) + \frac{1}{2c^2} \bar{g} (\varepsilon E^2 + \mu H^2) = \bar{0} \quad [\text{N/m}^3] \end{aligned} \quad (8)$$

The theory describes “Electromagnetic-Gravitational Interaction”, “Magnetic-Gravitational Interaction” and “Electric-Gravitational Interaction”. In this new theory particles do not interact with fields. The interaction between an electric charged particle and an electric field is not the interaction between a particle and a field but it is the interaction between the electric field of the particle interacting with the other electric field. Every interaction is an interaction between fields. Electric Fields interact with Electric Fields , Magnetic Fields interact with Magnetic Fields and Gravitational Fields only interact with Gravitational Fields. [Raymond J. Beach \(2014\)](#)

The consequence thereof is the dissemination of light (Electromagnetic Radiation) at the precise velocity of light ascertained by an Electro-Magnetic Perfect Equilibrium in all directions, at any given point, and at any temporal juncture. [Vegt Wim \(Calculation 1, June 21, 2022\)](#) posited this notion. This principle stands in opposition to Maxwell's theory of Electrodynamics, within which the speed of light is exclusively applicable to planar electromagnetic waves. [Maxwell James Clerk \(01 January 1865\)](#). The concept of the Universal Perfect Equilibrium transcends such limitations, applying to all manifestations of light, ranging from Laser Beams to the imagery depicting the genesis of the Universe.

2 “Gravitational RedShift/ BlueShift in “Light (EMR)” due to “Electromagnetic Gravitational Interaction”

To validate the New Theory, the experiment titled "Test of the Gravitational Redshift with Galileo Satellites in an Eccentric Orbit" was selected. [Herrmann Sven, Felix Finke, Martin Lülfi, Olga \(et al.\) \(4 December 2018\)](#) In this experiment, a stable MASER frequency from a ground station was transmitted to two Galileo Satellites. The frequency difference between the Ground Station and the Satellites was measured. This frequency shift was due to the gravitational field of the Earth, and two satellites were chosen to account for the eccentricity of the Galileo orbit.

Gravitational fields influence the propagation of electromagnetic radiation, specifically causing a phenomenon known as gravitational redshift. According to General Relativity, light or any form of electromagnetic radiation loses energy when it escapes a gravitational field, leading to an increase in wavelength and a corresponding decrease in frequency. In the "Test of the Gravitational Redshift" experiment, the MASER signal experiences this effect as it travels from the ground station (lower gravitational potential) to the satellites (higher gravitational potential). The difference in frequency recorded by the satellites is a direct measure of this redshift. By carefully selecting two satellites in slightly different orbits, the experiment compensates for the orbit's eccentricity, ensuring more precise measurements of the gravitational redshift. This effect highlights the interplay between gravity and electromagnetic radiation [Vegt Wim \(Calculation 3, August 25, 2022\)](#), confirming theoretical predictions with practical observations.

Assuming a gravitational field $g[z]$ depending on the radial direction in cartesian coordinates between the ground station and the satellites:

$$\overline{g[z]} = \left\{ 0, 0, \frac{G M_{Earth}}{4 \pi z^2} \right\} \quad (9)$$

In which G ($G = 6.67428 \cdot 10^{-11} \text{ Nm}^2 / \text{kg}^2$) equals the Gravitational constant, M_{Earth} the mass of the earth and r the radial distance from the centre of the earth. The mathematical solution [5] of equation (8) for plane electromagnetic waves (expressed in cartesian $\{x,y,z\}$ coordinates) related to the Electric Field Intensity equals:

$$\vec{E} = \begin{pmatrix} E_x \\ E_y \\ E_z \end{pmatrix} = \begin{pmatrix} e^{-\frac{G M_{Earth} \epsilon_0 \mu_0}{8 \pi z}} h \left[\omega_0 e^{-\frac{G M_{Earth} \epsilon_0 \mu_0}{4 \pi z}} (t - \sqrt{\epsilon \mu} z) \right] \\ 0 \\ 0 \end{pmatrix} \quad (10)$$

And the mathematical solution of (8) for the Magnetic Field Intensity equals:

$$\vec{H} = \begin{pmatrix} H_x \\ H_y \\ H_z \end{pmatrix} = \begin{pmatrix} 0 \\ \frac{1}{\sqrt{\epsilon_0 \mu_0}} e^{-\frac{G M_{Earth} \epsilon_0 \mu_0}{8 \pi z}} h \left[\omega_0 e^{-\frac{G M_{Earth} \epsilon_0 \mu_0}{4 \pi z}} (t - \sqrt{\epsilon \mu} z) \right] \\ 0 \end{pmatrix} \quad (11)$$

In this scenario, the initial frequency of the MASER radiation propagating in the direction of the Earth's gravitational field $g[z]$ is denoted by ω_0 . The inclusion of the exponential term indicates the Gravitational Redshift encountered as the MASER radiation traverses the Earth's gravitational field. While the speed of propagation of Electromagnetic Radiation (i.e., the speed of light) stays consistent, both the amplitude of the field intensity and the frequency undergo an exponential decline..

Mathematical calculations compare the results obtained from General Relativity with those from the New Theory. By setting the distance from the ground station to the Earth's centre as $z_1 = 6,378,000$ [m] (Earth's radius) and the average distance of ESA satellites in a Galileo orbit as $z_2 = 23,222,000$ [m] (distance from the ESA satellite to the Earth's centre), the Gravitational Redshift, [Delva P, Puchades N, Schönemann E, Dilssner F, Courde C et al \(December 2018\)](#) and [Herrmann Sven, Felix Finke, Martin Lülfi, Olga, et al \(December 2018\)](#), As per the principles established in General Relativity, this value is ascertained [Vegt Wim \(Calculation 2, July 16, 2023\)](#):

$$\Delta \omega_{GR} = 0.00000000004011815497097883 \text{ [s}^{-1}\text{]} \quad (12)$$

Calculated with Mathematica, the Gravitational RedShift [2, 5, 6, 17] according the New Theory, which is a solution of equation (8) equals [Vegt Wim \(Calculation 2, July 16, 2023\)](#):

$$\Delta \omega_{GR} = 0.00000000004011824206173742 \text{ [s}^{-1}\text{]} \quad (13)$$

Both calculated values are within the Range of the measured gravitational RedShift by the average values of both ESA satellites in the Galileo orbit

$$\Delta \omega_{\text{Measured}} = 0.000000000040118 \pm 2.2 \cdot 10^{-15} \text{ [s}^{-1}\text{]} \quad (14)$$

In [2] a factor α has been defined which presents the measured deviation α between the predicted Gravitational RedShift by General Relativity and the Measured Gravitational RedShift.

$$\alpha = \Delta \omega_{\text{MEASURED}} - \Delta \omega_{GR} = (2.2 \pm 1.6) \times 10^{-5} \quad (15)$$

A comparable factor α can be used to determine which theory (General Relativity or the New Theory) has the nearest approach to the experimentally measured data. Highly accurate measuring experiments are required with an accuracy higher than 16 digits beyond the decimal point.

3 Black Holes

3.1 Black Holes without Singularities with dimensions smaller than the diameter of the Hydrogen Atom

A second fundamental solution for equation (8) describes a Gravitational Electromagnetic Confinement (BLACK HOLE) [1] within a radial gravitational field with acceleration \bar{g} (in radial direction). This solution represents a Black Hole, the confinement of light due to its own gravitational field, and has no singularities. This solution for equation (8) describes Black Holes, dependent of time and radius, presenting discrete spherical energy levels, within a radial gravitational field with acceleration \bar{g} (in radial direction) has been represented in (16) and (17).

$$\begin{pmatrix} E_r \\ E_\theta \\ E_\phi \end{pmatrix} = \begin{pmatrix} 0 \\ f(r) \sin(kr) \sin(\omega t) \\ -f(r) \cos(kr) \cos(\omega t) \end{pmatrix} \quad \begin{pmatrix} H_r \\ H_\theta \\ H_\phi \end{pmatrix} = \sqrt{\frac{\epsilon}{\mu}} \begin{pmatrix} 0 \\ -f(r) \sin(kr) \cos(\omega t) \\ -f(r) \cos(kr) \sin(\omega t) \end{pmatrix} \quad \vec{g} = \begin{pmatrix} \frac{G_1}{4\pi r^2} \\ 0 \\ 0 \end{pmatrix} \quad (16)$$

$$w_{em} = \left(\frac{\mu_0}{2} (\vec{m} \cdot \vec{m}) + \frac{\epsilon_0}{2} (\vec{e} \cdot \vec{e}) \right) = f(r)^2 \left((\sin(kr) \sin(\omega t))^2 + (\cos(kr) \cos(\omega t))^2 + \frac{\epsilon}{\mu} (\sin(kr) \cos(\omega t))^2 + (\cos(kr) \sin(\omega t))^2 \right)$$

In which the radial function $f(r)$ equals:

$$f[r] = K e^{-\frac{G M_{BH} \epsilon_0 \mu_0}{8\pi r}} \quad (17)$$

G represents the Gravitational constant and M represents the total confined electromagnetic mass of the BLACK HOLE. Equation (16) presents a Standing (Confined) Electromagnetic Field Configuration with a phase shift of 90 degrees between the electric field and the magnetic field with the corresponding Nodes and AntiNodes. [13]. The solution has been calculated according [Newton's Shell Theorem](#).

Assuming a constant speed of light “ c ” and Planck's constant \hbar within the BLACK HOLE, the radius “ R ” (with $n = 1, 2, 3, 4, \dots$) of the BLACK HOLE with the energy of a proton, according $W = m_{proton} c^2$, would be: $1.5009211 \times 10^{-10}$ [J].

$$R_{GEON} = n \lambda = n \left(\frac{c}{f} \right) = n \left(\frac{c}{W} \right) \hbar = 7.1865 \cdot 10^{-26} \left(\frac{n}{W} \right) \quad (18)$$

$$R_{GEON} = n \cdot 3.82 \cdot 10^{-12} \text{ [m]}$$

Black Holes (GEONs) [Wheeler John Archibald \(15 January 1955\)](#) are varying from atomic dimensions with dimensions of 10^{-27} [kg], until Black Holes with dimensions of 10^{40} [kg]. At these dimensions Black Holes turn into Dark Matter. The fundamental boundary condition for the confinement of Electromagnetic radiation (BLACK HOLES) is that the energy flow (Poynting vector) $\vec{S} = \vec{E} \times \vec{H}$ equals zero at the surface of the confinement. This is possible at every “90 degrees Phase Shift Surface” (Sphere) between the Electric Field and the Magnetic Field.

3.1 Black Holes with a Singular point and Large dimensions

Fig 1 represents a Black Hole (GEON) [Wheeler John Archibald \(15 January 1955\)](#) with a mass of 10^{35} [kg] and a radius of about 25 [km] controlled by a different mathematical solution for equation (8). The radius of the Black Hole equals about 25 [km] which has been controlled by a different mathematical solution (19) for equation (8).

$$f[r] = K e^{\left(\frac{G M_{\text{BH}} \epsilon_0 \mu_0}{8 \pi r} - \log[r] \right)} \quad [\text{J} / \text{m}^3] \quad (19)$$

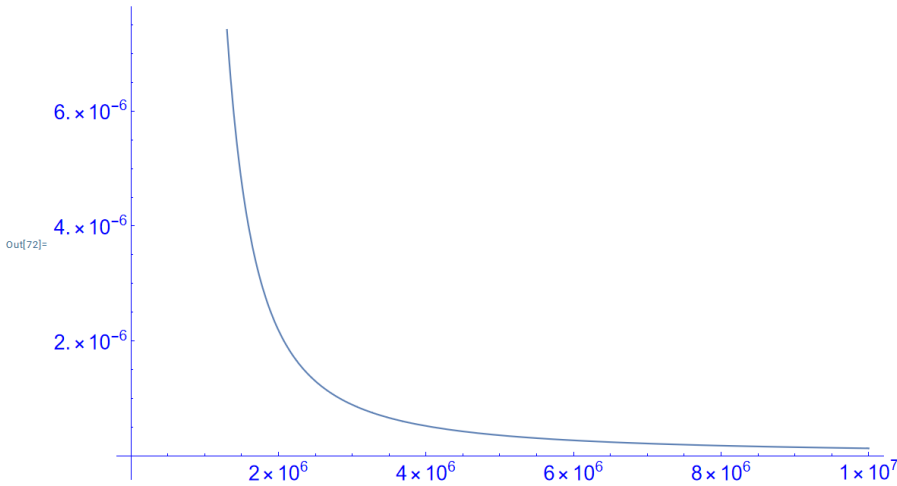


Fig. 1 The Energy Density [J/ m³] as a function of the Radius R = max 10⁷ [m] of the Black Hole.

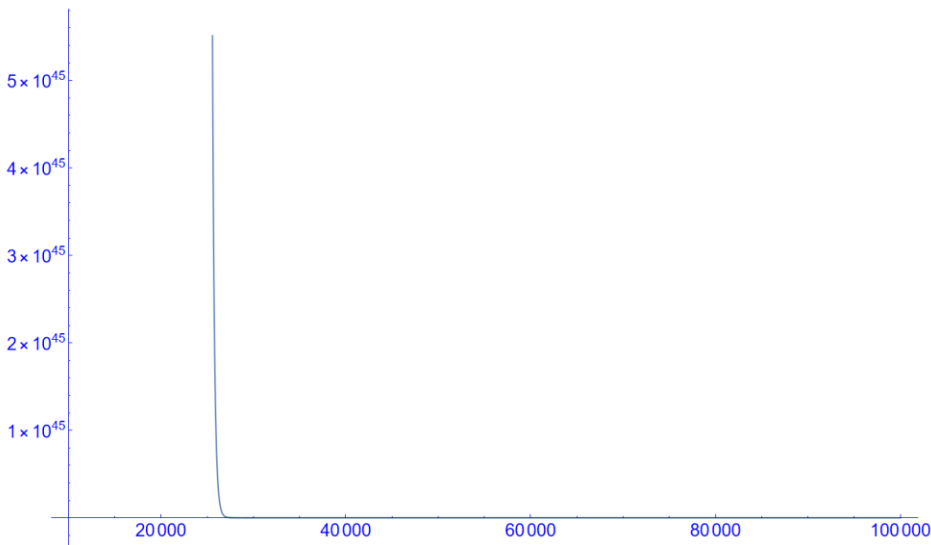


Fig. 2 The Energy Density [J/ m³] as a function of the Radius R = max 10⁵ [m]

Figure 1 and Figure 2 [Vegt Wim \(Calculation 4 21 February 2023\)](#) demonstrate the large effect of “Gravitational Intensity Shift” and “Gravitational RedShift” at the distance of 25 [km]. Over a distance of 10.000 [km] the intensity of the emitted light of the Black Hole with a mass of 10³⁵ [kg] falls back with a factor of 10⁻⁵¹. Also the frequency of the emitted light of the Black Hole falls back with a factor 10⁻⁵¹. Emitted light in the visible spectrum of 10¹⁴ [Hz] falls back to a frequency of 10⁻³⁷ [Hz]. These extreme low frequencies with extreme low intensities have never been measured which has result in the name “Black Hole” for the phenomenon of “Gravitational Intensity Shift” and “Gravitational RedShift” for a large mass. It follows from equation (8) and the solutions (10) and (11) that the speed of light does not change inside and around Black Hole. Only the direction of the propagation of light can change due to a gravitational. [Nikko John Leo S. Lobos, Reggie C. Pantig \(2022\)](#).

3.2 Dark Matter in the Universe controlled by “Gravitational Shielding”

Fig 3 represents Dark Matter with a total mass of 10^{53} [kg] and a radius of about 10 times the size of the Milky Way Galaxy. The radius [11] of the dark mass equals 5×10^{21} [m] which has been controlled by a different mathematical solution (20) for equation (8).

$$f[r] = K e^{\left(\frac{G M_{BH} \epsilon_0 \mu_0}{8 \pi r} - \log[r] \right)} \quad [J / m^3] \quad (20)$$

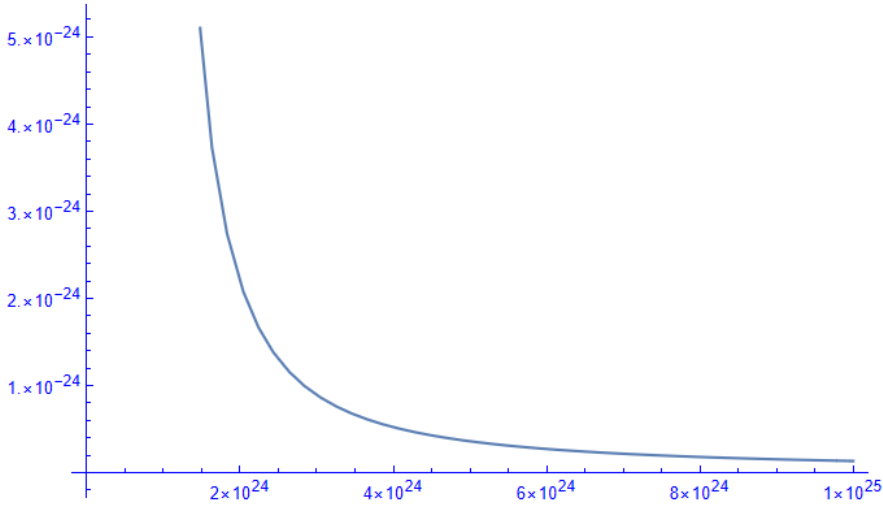


Fig. 3 The Energy Density [J/ m³] as a function of the Radius R = max 10²⁵ [m] of the Dark Matter.

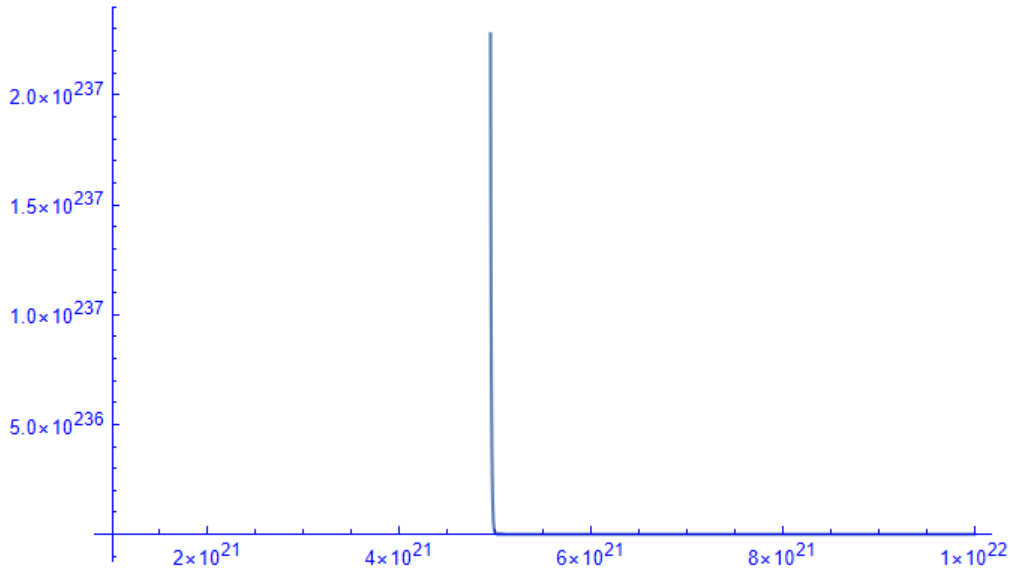


Fig. 4 The Energy Density [J/ m³] of the Dark Matter as a function of the Radius R = max 10²² [m]

Figure 3 and Figure 4 demonstrate the large effect of “Gravitational Intensity Shift” and “Gravitational RedShift” at the distance of $5 \cdot 10^{21}$ [m] which is 10 times the radius of the Milky Way Galaxy. Over the distance of $5 \cdot 10^{21}$ [m] the intensity of the emitted light of the Dark Matter with a mass of 10^{53} [kg] falls back with a factor of 10^{-261} . Also the frequency of the emitted light of the Black Hole falls back with a factor 10^{-261} . Emitted light in the visible spectrum of 10^{14} [Hz] falls back to a frequency of 10^{-247} [Hz]. These extreme low frequencies with extreme low intensities have never been measured which has result in the name “Dark Matter” for the phenomenon of “Gravitational Intensity Shift” and “Gravitational RedShift” for an extreme large mass. It follows from equation (8) and the solutions (10) and (11) that the speed of light does not change inside and around the Dark Mass. Only the direction of the propagation of light can change due to the gravitational field of the Dark Mass.

4 The relationship between Black Holes and Quantum Physics

Introducing the Quantum Vector Function $\bar{\phi}$,

$$\bar{\phi} = \sqrt{\frac{\mu}{2}} \left(\bar{H} + i \frac{\bar{E}}{c} \right) \quad (21)$$

Substituting (21) in (16) results in the quantum presentation for the BLACK HOLE:

$$\overline{\Phi(r, \theta, \varphi)} = \sqrt{\frac{\mu}{2}} \left(\bar{H} + i \frac{\bar{E}}{c} \right) f(r) \begin{pmatrix} \Phi_r \\ \Phi_\theta \\ \Phi_\varphi \end{pmatrix} \quad (22)$$

$$\overline{\Phi(r, \theta, \varphi)} = K \sqrt{\frac{\varepsilon}{\mu}} e^{-\frac{G I \varepsilon_0 \mu_0}{8 \pi r}} \begin{pmatrix} 0 & 0 & 0 \\ 0 & -\sin(k r) & \sin(k r) \\ 0 & -i \cos(k r) & i \cos(k r) \end{pmatrix} \begin{Bmatrix} 0 \\ \cos(\omega t) \\ i \sin(\omega t) \end{Bmatrix}$$

With “K” a constant value dependend of the mass of the BLACK HOLE. The Dot product between the unit vector and the Quantum Vector Function $\bar{\phi}$ represents the quantum mechanical probability function $\Psi[r, t]$ which is a fundamental solution of the Schrödinger Wave Equation [12].

$$\overline{\Phi(r, \theta, \varphi)} = K \sqrt{\frac{\varepsilon}{\mu}} e^{-\frac{G l \varepsilon_0 \mu_0}{8 \pi r}} \begin{pmatrix} 0 & 0 & 0 \\ 0 & -\sin(k r) & \sin(k r) \\ 0 & -i \cos(k r) & i \cos(k r) \end{pmatrix} \begin{Bmatrix} 0 \\ \cos(\omega t) \\ i \sin(\omega t) \end{Bmatrix} \quad (23)$$

$$\Psi(r, t) = \begin{Bmatrix} 1 & 1 & 1 \end{Bmatrix} \begin{Bmatrix} 0 \\ \cos(\omega t) \\ i \sin(\omega t) \end{Bmatrix} K \sqrt{\frac{\varepsilon}{\mu}} e^{-\frac{G l \varepsilon_0 \mu_0}{8 \pi r}} = K \sqrt{\frac{\varepsilon}{\mu}} e^{-\frac{G l \varepsilon_0 \mu_0}{8 \pi r}} e^{i \omega t}$$

The Scalar function $\Psi[r, t]$ represents a fundamental solution of the Quantum Mechanical Schrödinger wave equation. [12, 19, 36, 37]

4.1 Black Holes with Discrete Spherical Energy Levels at Sub-Atomic dimensions

In order to effectively confine Electromagnetic Energy, a critical requirement is that the Poynting vector reaches a value of zero at the surface of the spherical confinement. Creating this confinement within a sphere necessitates the presence of a standing electromagnetic wave pattern, characterized by concentric spheres. Each of these spheres establishes an antinodal plane for either the Electric Field (E) or the Magnetic Field (B), with the radius distance between each sphere precisely equal to half the wavelength of the overall confinement.

Within this setup, a constant denoted as "k" is introduced, defined as $k = n\pi/\lambda$, where "n" represents a natural number (1, 2, 3, 4, ...) and λ signifies the wavelength of the radiation. This equation elucidates the structured connection between the wavelength, the constant k, and the natural number n within the sphere of electromagnetic confinement in a spherical system.

4.1.1 Time and Radius dependent Black Holes with discrete Energy Levels. The confinements of Electromagnetic Radiation within spherical Regions.

Every concentric sphere represents an anti-nodal surface for the Electric Field (E) or the Magnetic Field (H). The Poynting Vector: $\vec{S} = \vec{E} \times \vec{H}$ at this spherical surface equals zero at any time and at any location at this sphere. The Electromagnetic Energy remains always within this sphere and the next concentric sphere. The concentric spheres have a difference in radius of one half wavelength of the electromagnetic radiation within the confinement and a different discrete energy level. Every concentric sphere represents an anti-nodal surface of the electric field or the magnetic field [11].

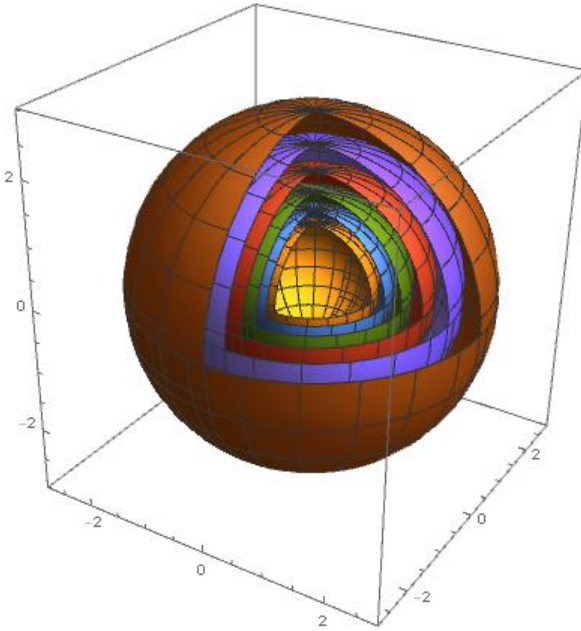


Fig. 5 Nodal and Antinodal Spheres for Standing (Confined) Spherical Electromagnetic waves with a 90 degrees phase shift between the Electric field and the Magnetic field. Equation (23)

Figure 5 illustrates the spatial distribution of nodal and antinodal spheres concerning stationary, confined spherical electromagnetic waves characterized by a distinctive 90-degree phase disparity between the electric and magnetic fields. This configuration is delineated by Equation (23) which encapsulates the nuanced interplay between these fundamental electromagnetic components within a three-dimensional framework [11].

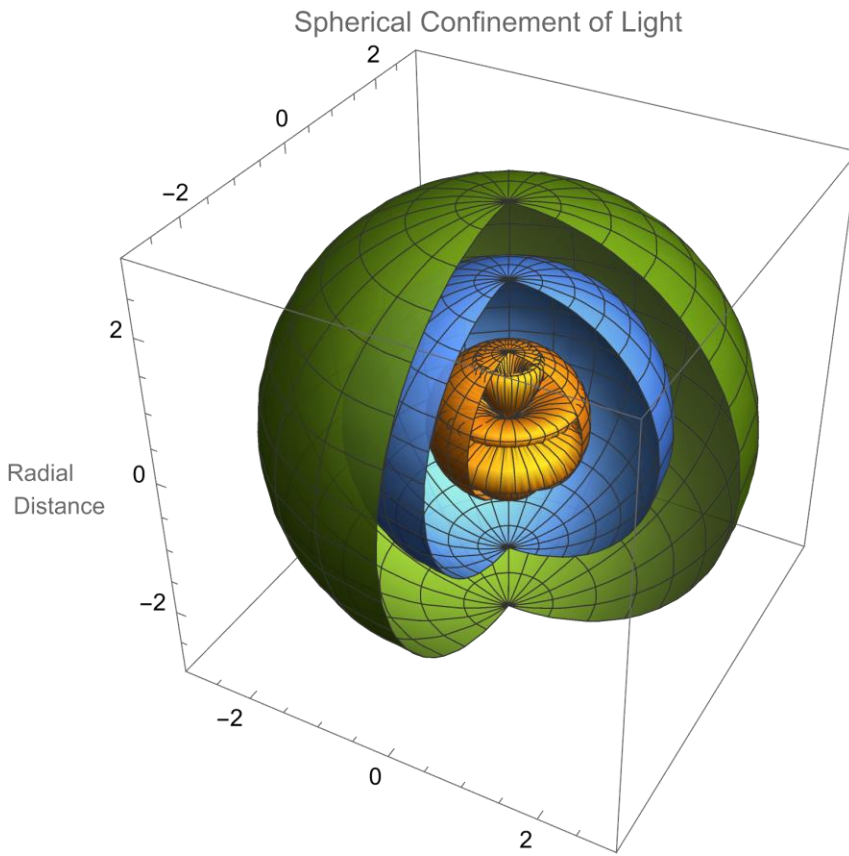


Fig. 6 Nodal- and Anti-nodal Spheres ($k = 3$) for Standing (Confined) Spherical Electromagnetic waves with a 90 degrees phase shift between the Electric field and the Magnetic field. Equation (23)

Figure 6 depicts the intricate nodal and anti-nodal spheres, emphasizing the scenario of standing, confined spherical electromagnetic waves where the wave number k is set at 3. [Vegt Wim \(Calculation 5, 16 March 2023\)](#) This visualization captures the unique 90-degree phase offset prevailing between the electric and magnetic fields. Equation (23) serves as the key mathematical representation encapsulating this phenomenon, further elucidating the interplay and characteristics of these electromagnetic waves within a specific spatial context.

Equation (24) describes a Time and Radius dependent BLACK HOLE.

$$\begin{aligned}\overline{\mathbf{E}} = & \mathbf{K} e^{-\frac{G1\epsilon_0\mu_0}{8\pi r}} \begin{pmatrix} 0 \\ \text{Sin}[k r] \text{Sin}[\omega t] \\ -\text{Cos}[k r] \text{Cos}[\omega t] \end{pmatrix} \\ & (24) \\ \overline{\mathbf{H}} = & \mathbf{K} e^{-\frac{G1\epsilon_0\mu_0}{8\pi r}} \sqrt{\frac{\epsilon_0}{\mu_0}} \begin{pmatrix} 0 \\ \text{Sin}[k r] \text{Cos}[\omega t] \\ -\text{Cos}[k r] \text{Sin}[\omega t] \end{pmatrix}\end{aligned}$$

Equation (20) represents by the function $\text{Sin}[k r]$ ($k = 1,2,3,4,\dots$) the confinement of electromagnetic radiation between two concentric spheres. \mathbf{K} represents the amplitude of the Electric/ Magnetic Field Intensty. [14]

4.1.2 Time and Polar Angle dependent Black Holes

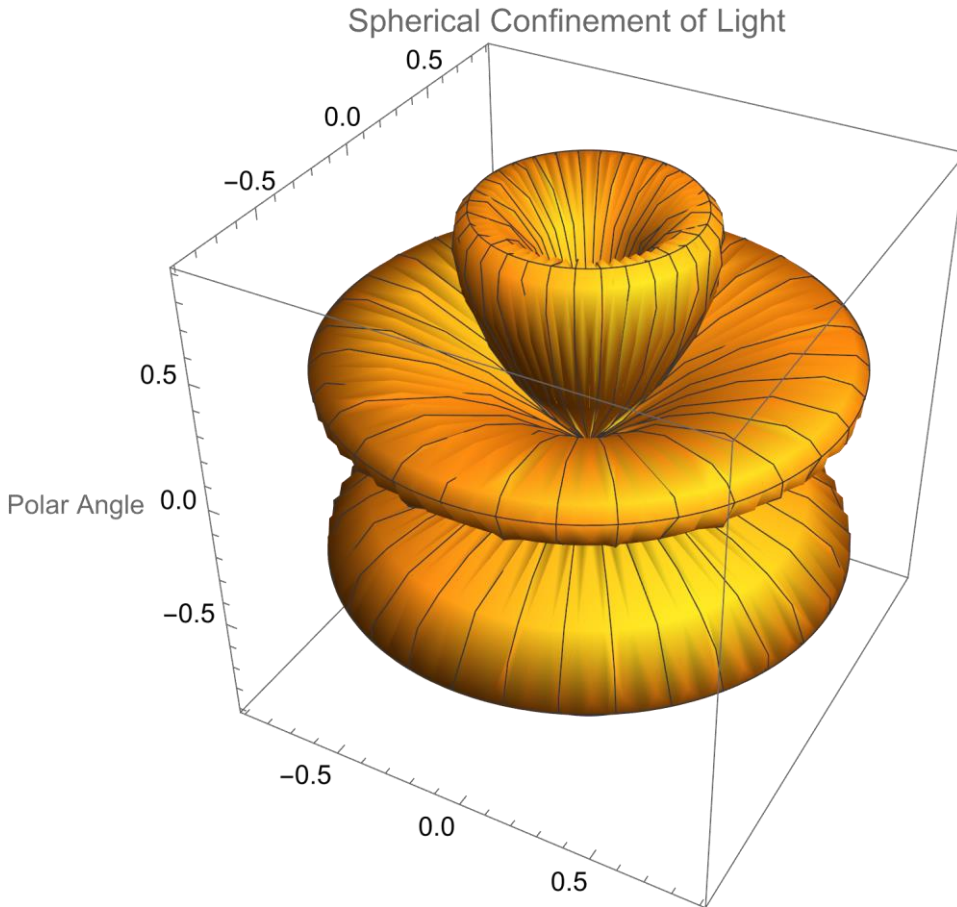


Fig. 7 Nodal- and Antinodal Polar Angle Regions ($m = 3$) for Standing (Confined) Spherical Electromagnetic waves with a 90 degrees phase shift between the Electric field and the Magnetic field. Equation (15)

In the realm of time and polar angle-dependent black holes, Section 4.1.2 explores the intricate dynamics associated with these celestial entities. Figure 7 offers a detailed insight into the nodal and antinodal regions across the polar angle, particularly emphasizing the case where the azimuthal quantum number m is defined as 3. [Vegt Wim \(Calculation 6, 23 April 2023\)](#) These findings shed light on the behavior of standing, confined spherical electromagnetic waves featuring a distinct 90-degree phase discrepancy between the electric and magnetic fields, as encapsulated by Equation (25). [13]

Equation (25) describes a Time and “Polar Angle” dependent BLACK HOLE [Vegt Wim \(Calculation 7, 15 May 2023\)](#):

$$\bar{E} = K e^{-\frac{G1\epsilon_0\mu_0}{8\pi r}} \begin{pmatrix} 0 \\ \sin[m \theta] \sin[\omega t] \\ \sin[m \theta] \cos[\omega t] \end{pmatrix} \quad (25)$$

$$\bar{H} = K e^{-\frac{G1\epsilon_0\mu_0}{8\pi r}} \sqrt{\frac{\epsilon_0}{\mu_0}} \begin{pmatrix} 0 \\ \sin[m \theta] \cos[\omega t] \\ -\sin[m \theta] \sin[\omega t] \end{pmatrix}$$

Equation (25) represents by the function $\sin[m \theta]$ ($m = 1, 2, 3, 4, \dots$) the confinement of electromagnetic radiation between two Polar Angular Regions [15].

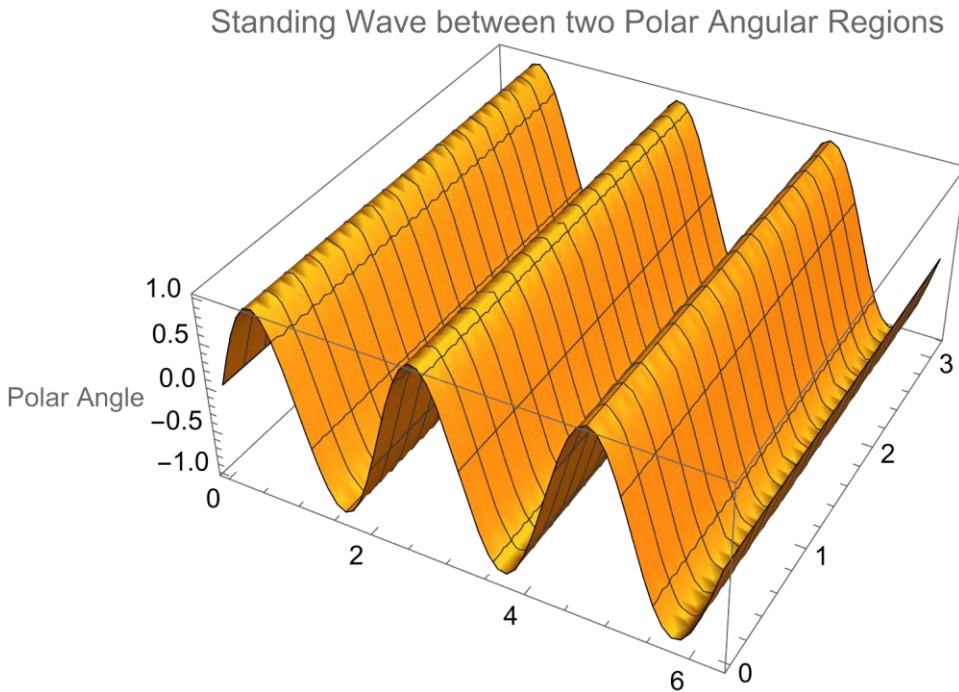


Fig. 8 Nodal- and Antinodal Polar Angle Regions ($m = 3$) for Standing (Confined) Electromagnetic waves with a 90 degrees phase shift between the Electric field and the Magnetic field. Equation (25)

Figure 8 illustrates the regions of nodal and antinodal behavior with respect to the polar angle, specifically focusing on cases where the azimuthal quantum number m is set to 3. This visualization pertains to standing, confined electromagnetic waves displaying a significant 90-degree phase differential between the electric and magnetic fields. The underlying dynamics are succinctly captured by Equation (15), providing a formal representation of these intriguing wave patterns.

4.1.3 Time and Azimuthal Angular dependent Black Holes

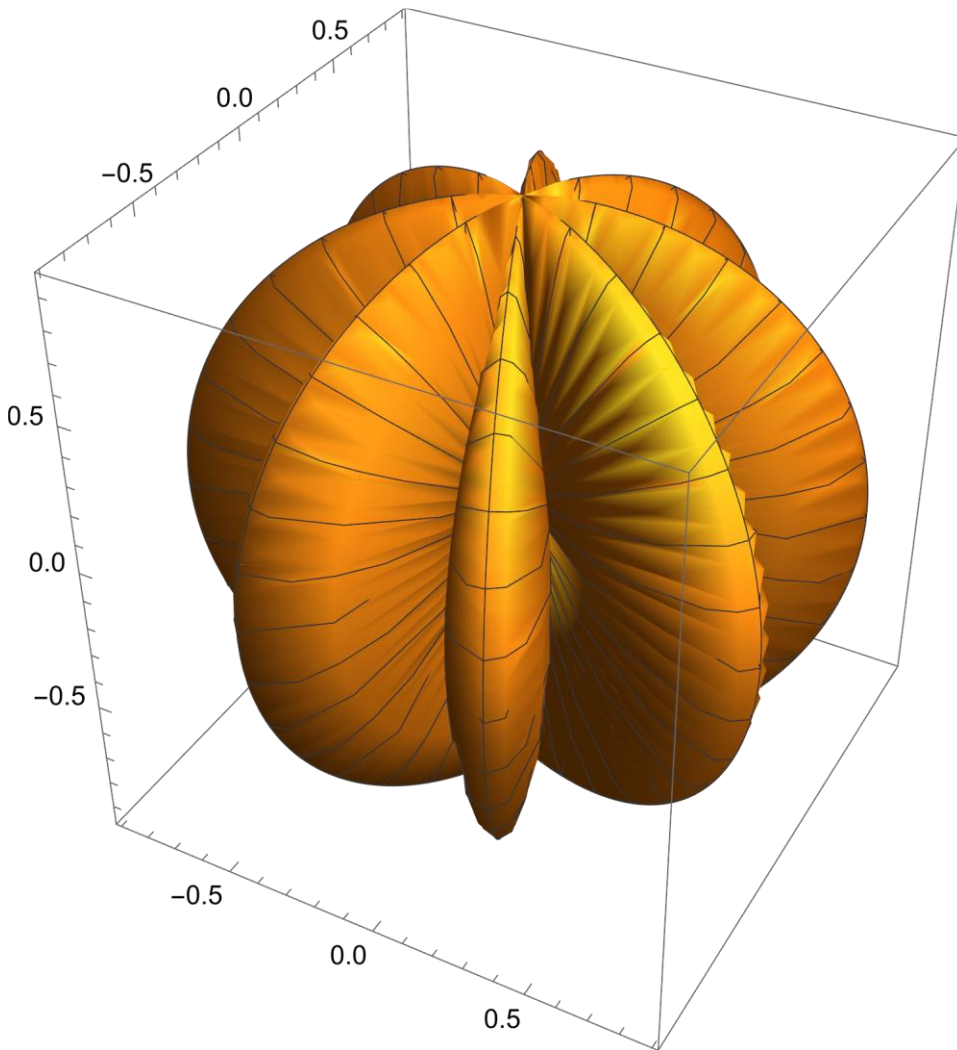


Fig. 9 Nodal- and Antinodal Azimuthal Angular Regions (n = 3) for Standing (Confined) Electromagnetic waves with a 90 degrees phase shift between the Electric field and the Magnetic field. Equation (26)

Fig. 9 Nodal- and Anti-nodal Azimuthal Angular Regions (n = 3) for Standing (Confined) Electromagnetic waves with a 90 degrees phase shift between the Electric field and the Magnetic field. Equation (26). Equation (26) describes a Time and “Polar Angle” dependent BLACK HOLE [Vegt Wim \(Calculation 7, 15 May 2023\)](#):

$$\bar{E} = K e^{-\frac{G1\epsilon_0\mu_0}{8\pi r}} \begin{pmatrix} 0 \\ \cos[n \varphi] \sin[\omega t] \\ \cos[n \varphi] \cos[\omega t] \end{pmatrix} \quad (26)$$

$$\bar{H} = K e^{-\frac{G1\epsilon_0\mu_0}{8\pi r}} \sqrt{\frac{\epsilon_0}{\mu_0}} \begin{pmatrix} 0 \\ \cos[n \varphi] \cos[\omega t] \\ -\cos[n \varphi] \sin[\omega t] \end{pmatrix}$$

The function denoted by Equation (26), where n ranges over integers (n = 1, 2, 3, ...), encapsulates the confinement of electromagnetic radiation within two distinct Azimuthal Angular Regions, as referenced by [14,15].

4.1.4 Time, Polar- and Azimuthal Angular dependent Black Holes

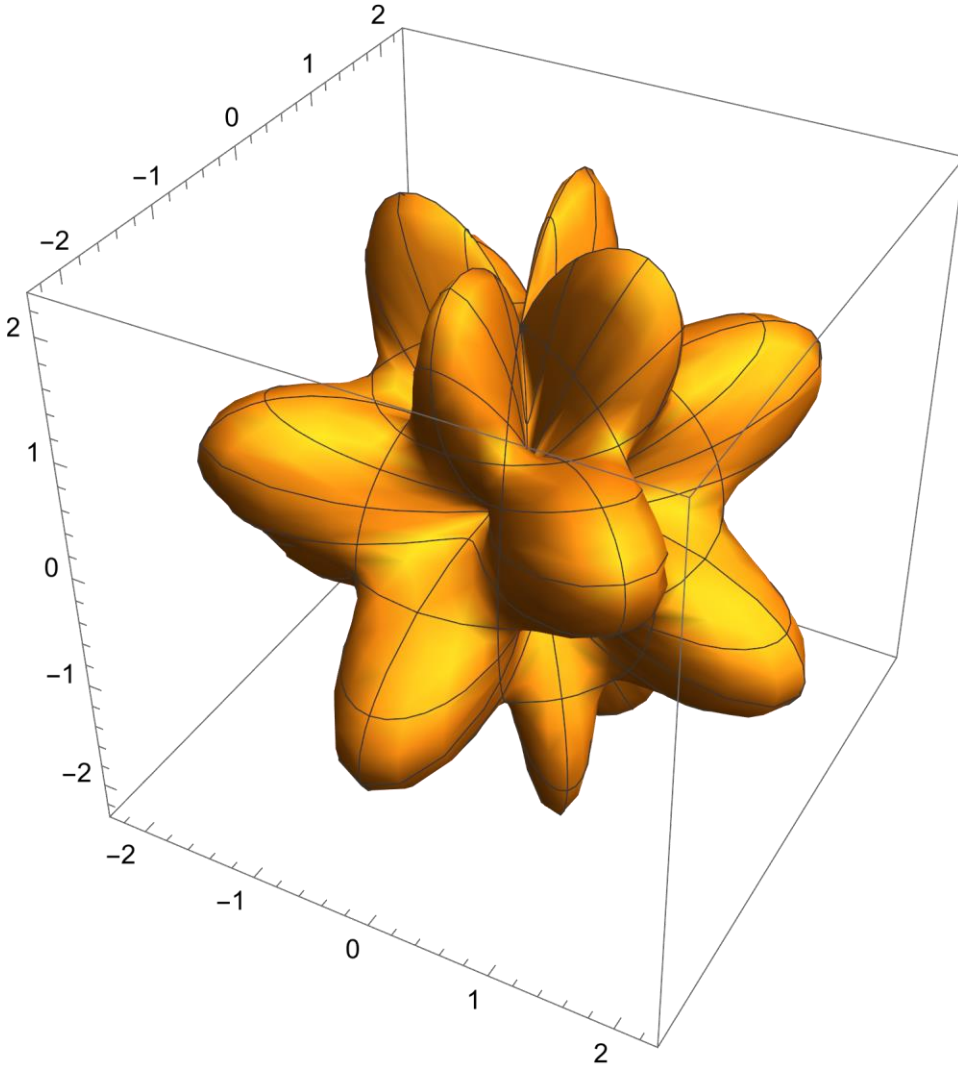


Fig. 10 Nodal- and Anti-nodal Polar Angular and Azimuthal Angular Regions ($n = 4$ and $m = 4$) for Standing (Confined) Electromagnetic waves with a 90 degrees phase shift between the Electric field and the Magnetic field. Equation (27)

Figure 10 showcases the delineation of nodal and anti-nodal regions pertaining to both polar and azimuthal angular domains, specifically when n is set to 4 and m is set to 4. This visualization sheds light on the intricate behavior of standing, confined electromagnetic waves characterized by a distinct 90-degree phase difference between the electric and magnetic fields. The mathematical framework governing

these phenomena is encapsulated by Equation (27), providing a formal expression of these electromagnetic wave patterns within the specified angular regions.

Equation (27) describes a Time “Azimuthal Angle” and “Polar Angle” dependent BLACK HOLE [Vegt Wim \(Calculation 7, 15 May 2023\)](#):

$$\begin{aligned} \vec{E} = K e^{-\frac{G1\epsilon_0\mu_0}{8\pi r}} & \begin{pmatrix} 0 \\ \cos[n \varphi] \sin[m \theta] \sin[\omega t] \\ \cos[n \varphi] \sin[m \theta] \cos[\omega t] \end{pmatrix} \\ \vec{H} = K e^{-\frac{G1\epsilon_0\mu_0}{8\pi r}} & \sqrt{\frac{\epsilon_0}{\mu_0}} \begin{pmatrix} 0 \\ -\cos[n \varphi] \sin[m \theta] \cos[\omega t] \\ \cos[n \varphi] \sin[m \theta] \sin[\omega t] \end{pmatrix} \end{aligned} \quad (27)$$

Equation (27) represents by the function $\cos[n \varphi]$ ($n = 1, 2, 3, 4, \dots$) and $\sin[m \theta]$ ($m = 1, 2, 3, 4, \dots$) the confinement of electromagnetic radiation between two Azimuthal Angular Regions and two Polar Angular Regions [14,15].

4.1.5 Spherical Confinement of Light between two Concentric Spheres within Black Holess

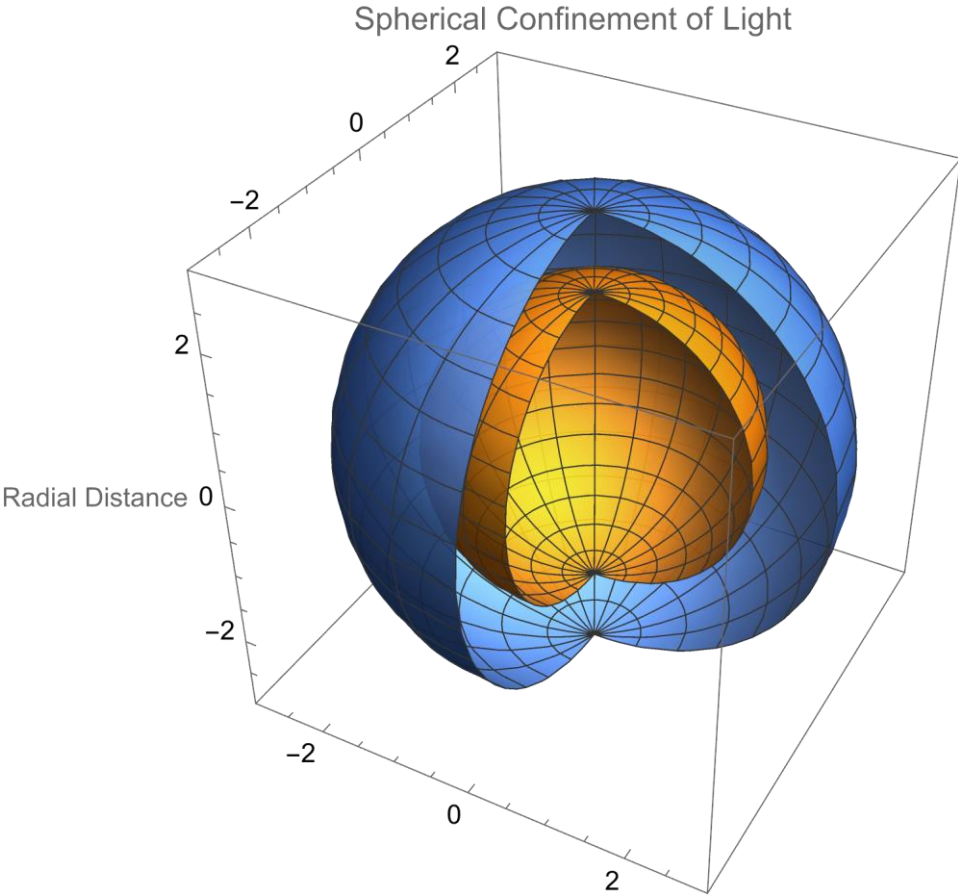


Fig.11 Nodal- and Antinodal Regions for Standing (Confined) Electromagnetic waves with a 90 degrees phase shift between the Electric field and the Magnetic field. Equation (14)

Figure 11 illustrates the nodal and antinodal regions associated with standing, confined electromagnetic waves featuring a 90-degree phase differential between the electric and magnetic fields. The intricacies of this wave behavior are represented mathematically by Equation (14), offering a formal description of the electromagnetic field dynamics within this context.

Equation (28) captures the phenomenon of the reflection of Confined Electromagnetic Energy within the confines of a Black Hole, delineated between two concentric spheres. In this scenario, the speed of light, which is contingent upon the

variable "r" representing the radial distance, undergoes a change in direction commensurate with the frequency of the confined light, or Electromagnetic Radiation.

Remarkably, a Black Hole possesses the capacity to undergo a process of splitting into two distinct Black Holes characterized by differing radii. During this transformation, the original Black Hole transitions to a lower energy level, akin to an atom descending to a lower energy state. The resultant new Black Holes formed as a consequence of this splitting represent the disparity in energy levels, resembling the analogous behavior of an atom transitioning between energy levels within its atomic structure. [Vegt Wim \(Calculation 5, 16 March 2023\)](#):

$$\begin{aligned}\bar{E} &= K e^{-\frac{G1\epsilon_0\mu_0}{8\pi r}} f \left[t - \frac{\sqrt{\epsilon_0 \mu_0} \cos[2 k r]}{2 k} \right] \begin{pmatrix} 0 \\ \sin[k r] \sin[\omega t] \\ -\cos[k r] \cos[\omega t] \end{pmatrix} \\ \bar{H} &= K e^{-\frac{G1\epsilon_0\mu_0}{8\pi r}} f \left[t - \frac{\sqrt{\epsilon_0 \mu_0} \cos[2 k r]}{2 k} \right] \sqrt{\frac{\epsilon_0}{\mu_0}} \begin{pmatrix} 0 \\ -\sin[k r] \cos[\omega t] \\ -\cos[k r] \sin[\omega t] \end{pmatrix}\end{aligned}\tag{28}$$

Spherical Confinement of Light between two Concentric Spheres

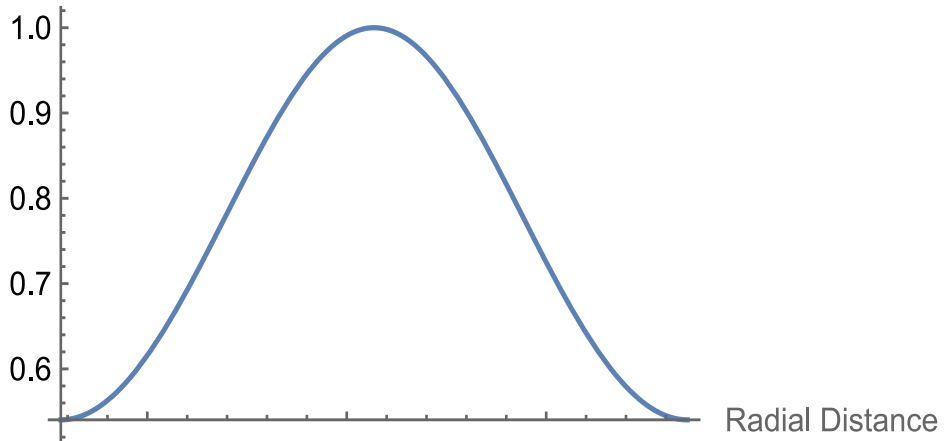


Fig. 12 Nodal- and Antinodal Regions for Standing (Confined) Electromagnetic within two concentric spheres. Equation (18)

Figure 12 presents a visual representation of the nodal and anti-nodal regions characterizing standing, confined electromagnetic waves enclosed within two concentric spheres. The electromagnetic field behaviors within this configuration are mathematically defined by Equation (18), offering a precise formulation of the wave dynamics within the specified spatial constraints. [12]

4.2 5

4.3 Universal Equilibrium in the “Concept of Quantum Mechanical Probability” in “The New Theory”.

The 4-dimensional notation for the divergence of the Stress-Energy Tensor (25) expresses in the 4th dimension (time dimension) the law of [Conservation of Energy](#). For an Electromagnetic Field the law for conservation of Energy has been expressed as:

$$\bar{f}^4 = \begin{pmatrix} f_4 \\ f_3 \\ f_2 \\ f_1 \end{pmatrix} = \square \cdot \bar{\bar{T}} = \begin{pmatrix} \nabla \cdot \bar{S} + \frac{\partial w}{\partial t} \\ f_3 \\ f_2 \\ f_1 \end{pmatrix} = \bar{0}^4 \quad (29)$$

From the equation for the “Conservation of Electromagnetic Energy” (38.1) the “Fundamental Equation for Confined Electromagnetic Interaction” in “The New Theory” will be derived, which equals the Relativistic Quantum Mechanical “Dirac” equation and the Schrödinger wave equation at velocities relative low compared to the speed of light.

The “Fundamental Equation for Confined Electromagnetic Interaction” in “The Proposed Theory” can be considered to be the relativistic version of the Quantum Mechanical Schrödinger wave equation, which equals the Quantum Mechanical Dirac Equation.

5.1 Confined Electromagnetic Energy within a 4-dimensional Equilibrium

The physical concept of quantum mechanical probability waves has been created during the famous [1927 5th Solvay Conference](#). During that period there were several circumstances which came just together and made it possible to create a unique idea of “**Material Waves**” (Solutions of Schödinger’s wave equation) being complex (partly real and partly imaginary) and describing the probability of the appearance of a physical object (elementary particle) generally indicated as “**Quantum Mechanical Probability Waves**”.

The idea of complex (probability) waves is directly related to the concept of confined ([standing](#)) waves. Characteristic for any [standing](#) acoustical wave is the fact that the Velocity and the Pressure (Electric Field and Magnetic Field in QLT) are always shifted over 90 degrees. The same principle does exist for the [standing \(confined\) electromagnetic waves](#),

For that reason every confined (standing) Electromagnetic wave can be described by a complex sum vector $\bar{\phi}$ of the Electric Field Vector \bar{E} and the Magnetic Field Vector \bar{B} (\bar{E} has 90 degrees phase shift compared to \bar{B}).

The vector functions $\bar{\phi}$ and the complex conjugated vector function $\bar{\phi}^*$ will be written as:

$$\bar{\phi} = \frac{1}{\sqrt{2} \mu} \left(\bar{B} + i \frac{\bar{E}}{c} \right) \quad (30)$$

\bar{B} equals the magnetic induction, \bar{E} the electric field intensity (\bar{E} has + 90 degrees phase shift compared to \bar{B}) and c the speed of light.

The complex conjugated vector function $\bar{\phi}^*$ equals:

$$\bar{\phi}^* = \frac{1}{\sqrt{2} \mu} \left(\bar{B} - i \frac{\bar{E}}{c} \right) \quad (31)$$

The dot product equals the electromagnetic energy density w :

$$\bar{\phi} \cdot \bar{\phi}^* = \frac{1}{2\mu} \left(\bar{\mathbf{B}} + i \frac{\bar{\mathbf{E}}}{c} \right) \cdot \left(\bar{\mathbf{B}} - i \frac{\bar{\mathbf{E}}}{c} \right) = \frac{1}{2} \mu H^2 + \frac{1}{2} \varepsilon E^2 = w \quad (32)$$

Using Einstein's equation $W = m c^2$, the dot product equals the electromagnetic mass density w :

$$\bar{\phi} \cdot \bar{\phi}^* \frac{1}{c^2} = \frac{\varepsilon}{2} \left(\bar{\mathbf{B}} + i \frac{\bar{\mathbf{E}}}{c} \right) \cdot \left(\bar{\mathbf{B}} - i \frac{\bar{\mathbf{E}}}{c} \right) = \frac{1}{2} \varepsilon \mu^2 H^2 + \frac{1}{2} \varepsilon^2 E^2 = \rho \text{ [kg/m}^3\text{]} \quad (33)$$

The cross product is proportional to the Poynting vector ([Ref. 3, page 202, equation 15](#)).

$$\bar{\phi} \times \bar{\phi}^* = \frac{1}{2\mu} \left(\bar{\mathbf{B}} + i \frac{\bar{\mathbf{E}}}{c} \right) \times \left(\bar{\mathbf{B}} - i \frac{\bar{\mathbf{E}}}{c} \right) = i \sqrt{\varepsilon \mu} \bar{\mathbf{E}} \times \bar{\mathbf{H}} = i \sqrt{\varepsilon \mu} \bar{\mathbf{S}} \quad (34)$$

This article presents a new “Gravitational-Electromagnetic Equation” describing Electromagnetic Field Configurations which are simultaneously the Mathematical Solutions for the Scalar Quantum Mechanical “Schrodinger Wave Equation” and more exactly the Mathematical Solutions for the Tensor representation of the “Relativistic Quantum Mechanical Dirac Equation” (41). [19]

The 4-dimensional divergence of the sum of the Electromagnetic Stress-Energy tensor expresses the 4-dimensional Force-Density vector (expressed in $[\text{N/m}^3]$ in the 3 spatial coordinates) as the result of Electro-Magnetic-Gravitational interaction.

$$f^\mu = \partial_\nu T^{\mu\nu} = 0 \quad (35)$$

In vector notation the 4-dimensional Force-Density vector can be written as:

$$\bar{f}^4 = \begin{pmatrix} f_4 \\ f_3 \\ f_2 \\ f_1 \end{pmatrix} = \square \cdot \bar{\mathbf{T}} = 0 \quad (36)$$

The fundamental boundary condition for this alternative approach to gravity is the requirement that the Force 4 vector equals zero in the 4 dimensions, expressing a universal 4-dimensional equilibrium:

The 3 spatial components of the Force-Density vector, as a result of Electro-Magnetic-Gravitational interaction can be written as:

Substituting the electromagnetic values for the electric field intensity “E” and the magnetic field intensity “H” in (36) results in the 4-dimensional representation of the Electro-Magnetic-Gravitational Fields Equation (37):

$$\begin{aligned}
 & \text{Energy-Time Domain} \\
 (f_4) \quad & \Leftrightarrow \nabla \cdot (\bar{E} \times \bar{H}) + \frac{1}{2} \frac{\partial \left(\epsilon_0 (\bar{E} \cdot \bar{E}) + \mu_0 (\bar{H} \cdot \bar{H}) \right)}{\partial t} = 0 \\
 & \text{3-Dimensional Space Domain} \tag{37} \\
 \begin{pmatrix} f_3 \\ f_2 \\ f_1 \end{pmatrix} \quad & \Leftrightarrow -\frac{1}{c^2} \frac{\partial (\bar{E} \times \bar{H})}{\partial t} + \epsilon_0 \bar{E} (\nabla \cdot \bar{E}) - \epsilon_0 \bar{E} \times (\nabla \times \bar{E}) \\
 & + \mu_0 \bar{H} (\nabla \cdot \bar{H}) - \mu_0 \bar{H} \times (\nabla \times \bar{H}) = \bar{0}
 \end{aligned}$$

In which f_1 , f_2 , f_3 , represent the force densities in the 3 spatial dimensions and f_4 represent the force density (energy flow) in the time dimension (4th dimension). Equation (37) can be written as:

$$\begin{aligned}
 & \text{Energy-Time Domain} \\
 & \text{Conservation of Energy} \\
 & \text{B-7} \\
 (f_4) \quad & \nabla \cdot \bar{S} + \frac{\partial w}{\partial t} = 0 \tag{38.1} \\
 & \text{3-Dimensional Space Domain} \\
 & \tag{38} \\
 & \begin{array}{ccc} \text{B-1} & \text{B-2} & \text{B-3} \\ -\frac{1}{c^2} \frac{\partial (\bar{E} \times \bar{H})}{\partial t} & + \epsilon_0 \bar{E} (\nabla \cdot \bar{E}) - \epsilon_0 \bar{E} \times (\nabla \times \bar{E}) & + \\ \text{B-4} & \text{B-5} & \\ + \mu_0 \bar{H} (\nabla \cdot \bar{H}) - \mu_0 \bar{H} \times (\nabla \times \bar{H}) & = \bar{0} & \end{array} \tag{38.2} \\
 \begin{pmatrix} f_3 \\ f_2 \\ f_1 \end{pmatrix}
 \end{aligned}$$

The 4th term in equation (38.1) can be written in the terms of the Poynting vector “S” and the energy density “w” representing the electromagnetic law for the conservation of energy (Newton’s second law of motion).

5.3 The 4-dimensional Relativistic Dirac Equation

Substituting (32) and (34) in Equation (38.1) results in The 4-Dimensional Tensor presentation for the relativistic quantum mechanical Dirac Equation (39):

$$\begin{aligned}
 (x_4) \quad & \nabla \cdot (\bar{\phi} \times \bar{\phi}^*) + \frac{i}{c} \frac{\partial \bar{\phi} \cdot \bar{\phi}^*}{\partial t} = 0 \\
 \begin{pmatrix} x_3 \\ x_2 \\ x_1 \end{pmatrix} \quad & \frac{i}{c} \frac{\partial (\bar{\phi} \times \bar{\phi}^*)}{\partial t} - \left(\bar{\phi} \times (\nabla \times \bar{\phi}^*) + \bar{\phi}^* \times (\nabla \times \bar{\phi}) \right) + \left(\bar{\phi} (\nabla \cdot \bar{\phi}^*) + \bar{\phi}^* (\nabla \cdot \bar{\phi}) \right) = 0
 \end{aligned} \tag{39}$$

To transform the electromagnetic vector wave function $\bar{\phi}$ into a scalar (spinor or one-dimensional matrix representation), the Pauli spin matrices σ and the following matrices (Ref. 3 page 213, equation 99) are introduced:

$$\bar{\alpha} = \begin{bmatrix} 0 & \sigma \\ \sigma & 0 \end{bmatrix} \quad \text{and} \quad \bar{\beta} = \begin{bmatrix} \delta_{ab} & 0 \\ 0 & -\delta_{ab} \end{bmatrix} \tag{40}$$

The Equations (6), (32) and (34) can be written in tensor presentation as the 4-Dimensional Relativistic Quantum Mechanical Dirac Equation: [3] (Equation 102, page 213)

$$(x_4) \quad \left(\frac{i m c}{h} \bar{\beta} + \bar{\alpha} \cdot \nabla \right) \psi = - \frac{1}{c} \frac{\partial \psi}{\partial t} \tag{41.1}$$

$$\begin{aligned}
 \begin{pmatrix} x_3 \\ x_2 \\ x_1 \end{pmatrix} \quad & - \frac{1}{c^2} \frac{\partial (\bar{\mathbf{E}} \times \bar{\mathbf{H}})}{\partial t} + \varepsilon_0 \bar{\mathbf{E}} (\nabla \cdot \bar{\mathbf{E}}) - \varepsilon_0 \bar{\mathbf{E}} \times (\nabla \times \bar{\mathbf{E}}) + \\
 & + \mu_0 \bar{\mathbf{H}} (\nabla \cdot \bar{\mathbf{H}}) - \mu_0 \bar{\mathbf{H}} \times (\nabla \times \bar{\mathbf{H}}) + \gamma_0 \bar{\mathbf{g}} (\nabla \cdot \bar{\mathbf{g}}) - \gamma_0 \bar{\mathbf{g}} \times (\nabla \times \bar{\mathbf{g}}) = \bar{0}
 \end{aligned} \tag{41.2}$$

6. The fundamental experiment to validate the New Theory in Physics

The fundamental foundation for Einstein's Theory of General Relativity is the "Curvature of Space and Time" due to a Gravitational Field. In the "Theory of General Relativity" Gravitational RedShift has been explained by a change in time and space resulting is a change in the observed frequency shift in the spectrum of the light being emitted by far away Galaxies. The foundation for Einstein's theory of General Relativity is a constant value for the speed of light in the absence of a gravitational field.

In the "New Theory" the fundamental foundation is "Equilibrium". Equilibrium for the "5 fundamental force densities in light" in any direction at any time and at any location. The 5 fundamental forces in light are:

- 1) "Inertia Force" (Energy has always inertia according Einstein's $E = m c^2$)
- 2) "Electric Force"
- 3) "Magnetic Force"
- 4) "Electric Force" due to the "Lorentz Transformation" of the "Magnetic Force"
- 5) "Magnetic Force" due to the "Lorentz Transformation" of the "Electric Force"

The speed of light has been fully controlled by the perfect equilibrium between the 5 fundamental force densities in any direction at any time and at any location. For a single beam of light the perfect equilibrium between the 5 fundamental forces always results in the speed of light:

$$c = 1 / \sqrt{\epsilon \mu} \quad (42)$$

However in this experiment 3 beams of light with the same frequency and the same phase and 3 controllable (LPA) different intensities K1, K2 and K3 will cross each other in 3 orthogonal directions. This will result in different boundary conditions for the total electromagnetic radiation and will be measurable by a changing in the speed of light. In this experiment by a changing of the speed of light in the chosen z-direction. The changing of the speed of light will become visible by a change in the interference patterns of the 2 LASER beams. The original beam and the manipulated beam.

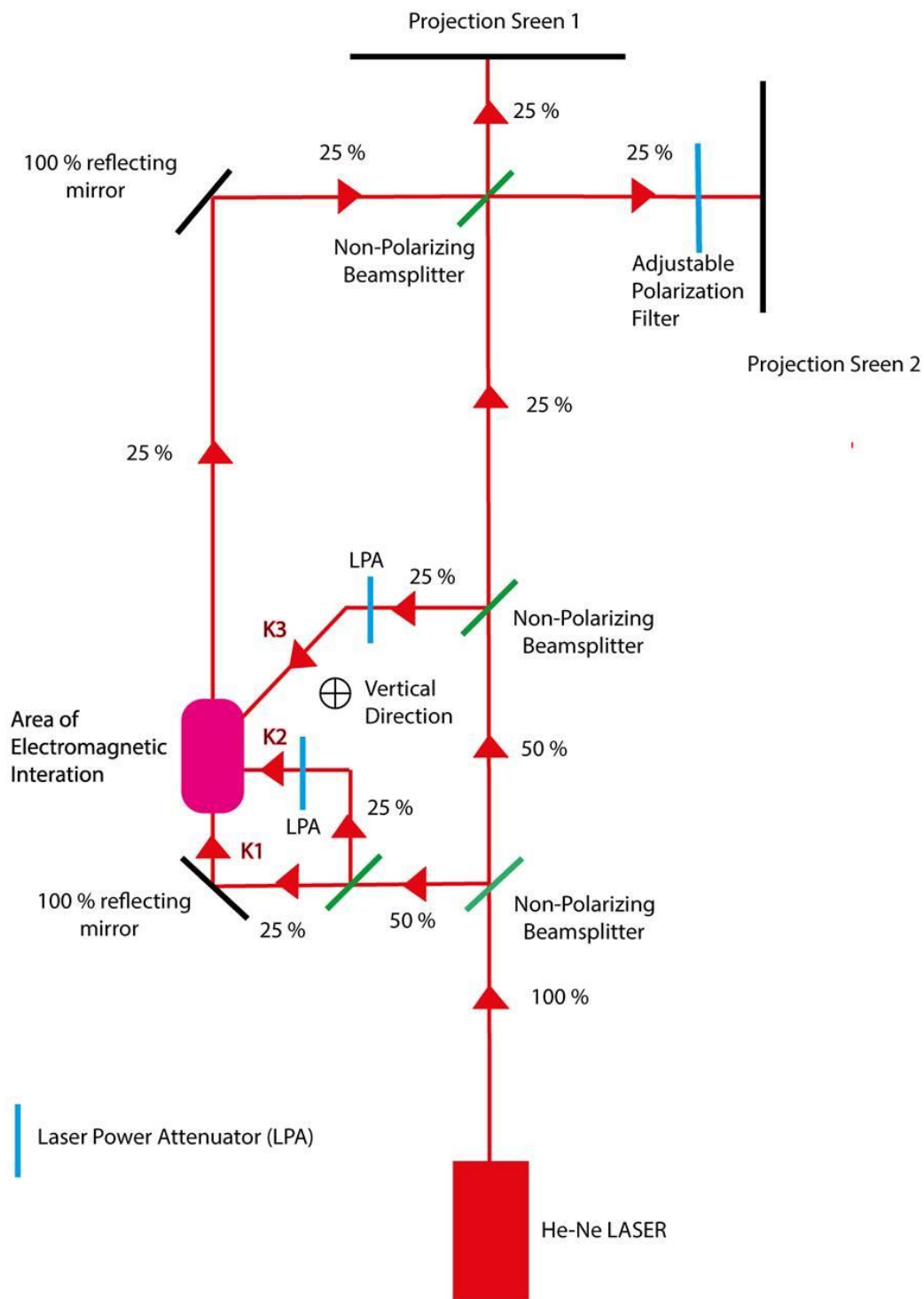
The solution for equation (8) has been calculated in Mathematica when 3 laser beams cross each other perpendicular and will cause a change in the speed of light within the intersection of the 3 crossing Laser Beams due to Electromagnetic Interaction.

According the calculations in Mathematica 11.3 at the exact “**location dependent speed of light $c[x,y,z]$** “ there will be a perfect equilibrium between all the electromagnetic- inertia- and radiation pressure force densities at any time in any direction:

$$\frac{1}{c(x,y,z)} = h[x,y,z] = \frac{(K_2^2 x - K_1 K_3 x + K_3^2 y + K_1^2 z - K_2 (K_1 y + K_3 z))}{K_1^2 + K_2^2 + K_3^2} \sqrt{\epsilon_0} \sqrt{\mu_0} \quad (43)$$

The result in equation (43) has been presented in [Vegt Wim, Calculation 8 \(16 June 2024\)](#). The change in the speed of light in the cross section will become visible in the interference patterns on screen 1 and screen 2 by changing the intensity of the secondary and third LASER beams by the two “[LASER Power Attenuators](#)” (indicated in blue) after passing the [beamsplitter\(s\)](#).

Technical Setup for the Experiment to demonstrate that the speed of light will change in the area of Electromagnetic Interaction



6. Conclusions

- General Relativity, founded on the zero rest mass of photons, elucidates the interplay between Gravity and Light within a 4-dimensional spacetime curvature induced by gravitational fields, guiding the path of light through the curved geometry.
- The new theory proposes a dual separation between mass and inertia for light (photons): inertia solely exists along the beam's propagation direction, determining light speed, while mass exists perpendicularly to the propagation and influences light deflection by gravitational fields.
- Black Holes, representing gravitational-electromagnetic confinements, are solutions of the relativistic quantum mechanical Dirac equation, showcasing the profound impacts of Gravitational Intensity Shift and Gravitational RedShift. Detecting these phenomena requires extremely sensitive observatories at low frequency levels.
- The new theory explores the role of "CURL" within gravitational fields near Black Holes, affecting Gravitational Lensing in a manner unexplained by General Relativity.
- Within a 4-dimensional equilibrium and considering force densities, Black Holes at sub-atomic scales emerge as physical realities, offering solutions to the Relativistic Quantum Mechanical Dirac Equation with discrete energy levels.
- Experimental validation comparing Gravitational RedShift calculations between General Relativity and the new theory in Earth's gravitational field, though challenging, necessitates high accuracy instruments.
- Dark Matter's existence is substantiated by the gravitational effects of Gravitational RedShift and Gravitational Intensity Shift, rendering galaxies invisible beyond a certain gravitational shielding distance due to mass-induced effects on light emission.
- The experiment to verify the new theory's predictions is underway, with results yet to be published pending thorough examination by multiple scientific institutions to ascertain the implications of observed interference pattern fluctuations. The collaborative effort of global scientific teams is vital for the comprehensive evaluation of these experimental findings

5.1 Data Availability

All Data and Calculations have been published at:

<https://quantumlight.science/>

References

- Delva P, Puchades N, Schönemann E, Dilssner F, Courde C (et. all); Gravitational Redshift Test Using Eccentric Galileo Satellites; Phys. Rev. Lett. 121, 231101 – Published 4 December 2018; DOI: [10.1103/PhysRevLett.121.231101](https://doi.org/10.1103/PhysRevLett.121.231101)
- Einstein Albert; On the Influence of Gravitation on the Propagation of Light; Annalen der Physik (ser. 4), **35**, 898–908, http://myweb.rz.uni-augsburg.de/~eckern/adp/history/einstein-papers/1911_35_898-908.pdf
- Einstein Albert; “Elementare Überlegungen zur Interpretation der Grundlagen der Quanten-Mechanik”; published in 1953 (Oliver and Boyd), pages 33-40; Translated into English, 2011, DOI: <https://doi.org/10.48550/arXiv.1107.3701>
- Herrmann Sven, Felix Finke, Martin Lulf, Olga (et. Al.) I; Test of the Gravitational Redshift with Galileo Satellites in an Eccentric Orbit ;Phys. Rev. Lett. **121**, 231102 – Published 4 December 2018; Gravitational Redshift Test Using Eccentric Galileo Satellites, DOI: [10.1103/PhysRevLett.121.231102](https://doi.org/10.1103/PhysRevLett.121.231102)
- Maxwell James Clerk; A dynamical theory of the electromagnetic field; 01 January 1865; <https://royalsocietypublishing.org/doi/10.1098/rstl.1865.0008>
- Nikko John Leo S. Lobos, Reggie C. Pantig; Generalized Extended Uncertainty Principle Black Holes: Shadow and lensing in the macro- and microscopic realms; Physics 2022, 4(4), 1318-1330; <https://doi.org/10.3390/physics4040084>
- Raymond J. Beach; A classical Field Theory of Gravity and Electromagnetism; Journal of Modern Physics; 2014, 5, 928-939
- Vegt Wim; A Continuous Model of Matter based on AEONs, Physics Essays, Volume 8, Number 2, 1995; Equation 119 Page 216, Equation A45 Page 221 and Equation A46 Page 221; DOI: [10.31219/osf.io/ra7ng](https://doi.org/10.31219/osf.io/ra7ng)
- Vegt Wim; The 4-Dimensional Dirac Equation in Relativistic Field Theory; Equation 23 Page 49; 2-Oct-2021; DOI: [10.14738/aivp.91.9403](https://doi.org/10.14738/aivp.91.9403)
- Vegt Wim; [The Origin of Gravity; Research & Reviews: Journal of Pure and Applied Physics](#); Manuscript No. JPAP-22-76022(A); Equation 21 Page 13; Published: 26-Oct-2022; DOI: [10.4172/2320-2459.10004](https://doi.org/10.4172/2320-2459.10004).
- Vegt Wim; The speed of light by Electromagnetic Interaction; Calculation 1; 21 June 2022; https://community.wolfram.com/groups/-/m/t/2576692?p_p_auth=mTldHX3v
- Vegt Wim; Gravitational RedShift between two Atomic Clocks, Calculation 2; 16 July 2023; https://community.wolfram.com/groups/-/m/t/2622560?p_p_auth=EC8QO0Xz

Vegt Wim; Propagation of Light within a Gravitational Field in Quantum Light Theory, Calculation 3; 25 August 2022; <https://community.wolfram.com/groups/-/m/t/2576537>

Vegt Wim; Black Holes with Discrete Spherical Energy Levels, Calculation 4; 21 February 2023; https://community.wolfram.com/groups/-/m/t/2896941?p_p_auth=D7ZKuo3k

Vegt Wim; Time and Radius dependent GEONs with discrete Energy Levels, Calculation 5; 16 March 2023; https://community.wolfram.com/groups/-/m/t/2991686?p_p_auth=CGtF3Tkg

Vegt Wim; Time and Polar Angular Regions dependent GEONs with discrete energy levels, Calculation 6; 23 April 2023; https://community.wolfram.com/groups/-/m/t/2901457?p_p_auth=H4jjDHmQ

Vegt Wim; Time and Azimuthal Regions dependent GEONs with discrete energy levels, Calculation 7; 15 May 2023; https://community.wolfram.com/groups/-/m/t/3200586?p_p_auth=TWz8jyxO

Vegt Wim; An Experiment to test General Relativity: Changing the speed of light by Electromagnetic Interaction, Calculation 8; 16 June 2024; https://community.wolfram.com/groups/-/m/t/3168232?p_p_auth=425V1HDh

Vegt Wim; “The Origin of Gravity in “Quantum Light Theory””; OSF Preprints; 14 October 2022; DOI: [10.31219/osf.io/n43yd](https://doi.org/10.31219/osf.io/n43yd)

Vegt Wim; The Origin of Gravity, A second order Lorentz Transformation for "Accelerated Electromagnetic Fields", Generating a Gravitational Field and the property of Mass, International Research Journal of Pure and Applied Physics [Vol.9 No.1, pp.12-52, 2022](#).

Vegt Wim; The 4-Dimensional Dirac Equation in Relativistic Field Theory, European Journal of Applied Sciences, [Vol 9, No. 1, pp 35 – 93, 2021](#)

[20] Vegt Wim; A Perfect Equilibrium inside a Black Hole; Wolfram Community: https://community.wolfram.com/groups/-/m/t/3087823?p_p_auth=dpH7iBMg

Weng Zihua, Influence of velocity curl on conservation laws, October 2008, <https://doi.org/10.48550/arXiv.0810.0065>

Wheeler John Archibald; GEONs, Physical Review Journals Archive, 97, 511, Issue 2, pages 511-526, Published 15 January 1955, Publisher: American Physical Society, [DOI: 10.1103/PhysRev.97.511](https://doi.org/10.1103/PhysRev.97.511):